Department of Physics and Astronomy
University of Heidelberg

Bachelor Thesis in Physics
submitted by

Vincent C. Mader

born in Ulm (Germany)

February 2020

Gas accretion onto eccentric planets

This Bachelor Thesis has been carried out by Vincent C. Mader at the
Max Planck Institute for Astronomy in Heidelberg
under the supervision of
Dr. Bertram Bitsch

Abstract

- eccentric planets not often investigated
- look at planet formation processes for different eccentricities
- The goal of this thesis is to investigate the interaction between a planet's gas accretion rate and the eccentricity of its orbit.
- for differently sized planets and several different disks
-

Zusammenfassung

Acknowledgements

Contents

List of Figures

Chapter 1

Introduction

1.1 Historical Context (better section name?)

As early as the time of the ancient Babylonian civilization, several bright objects could be distinguished from the rest of the the night sky. In contrast to the stars, which on human timescales constitute a relatively static background, these objects seemed to exhibit independent motion across the sky. This explains why the word we use today to describe these objects is *planet*, which has its origin in the ancient Greek *planetes*, literally meaning "wanderer".

It was observed that every now and then, the movement of these sources of light seemed to stop and then reverse for a while. Nowadays, we of course know that this behavior is explained by the planets' independent motion around the Sun. Although it was suggested that the Earth does not make up the center of the universe relatively early, e.g. by Aristarchus of Samos in the third century B.C.E., this was not a widely accepted fact until relatively recent times.

Up until the Renaissance, the widespread world view followed a model most notably suggested by the Greek polymath Ptolemy, who argued for a geocentric universe, where the Sun, planets and stars all orbit the Earth. Each of the orbiting planets was thought to additionally travel on a so-called epicycle, which helped explain the fact that the observed planets did not always travel in the same direction as seen from Earth.

Due to their low apparent magnitudes, the planets Mercury, Venus, Mars, Jupiter and Saturn can be observed from Earth with the naked eye. Thus, they were known to most historic societies with any interest in astronomy. Not being able to explain their origin, humans in civilizations all over the world tried to give these mysterious sources of light meaning by incorporating them into their stories, mythologies and religions.

It would take almost two millenia before the heliocentric model of the solar system gained widespread attention. In the 16th century, the Polish polymath Nicolaus Copernicus formulated a model of the universe with the Sun at its center and the planets traveling around it on concentric circles. Eventually, the observations of Mars' orbit done by Johannes Kepler and his mentor Tycho Brahe lead to the first mathematical description (?) of the motions of astronomical bodies. Kepler's ideas improved on the model of Copernicus. Instead of circles, Kepler realized that the planets move around the sun on ellipses, with the Sun positioned at one of the ellipse's foci.

These observations would lead Isaac Newton to formulate his theory of gravity together with his laws of motion which, it could be argued, marked the start of the scientific revolution that would take place in the following centuries. He regognized that this law suffices to correctly predict the motions of the astronomical bodies. Additionally, he noticed that this same law held true not only

for the planets, but also for any falling object here on Earth. (first scientific law?).

The new, heliocentric world view provided a lot of new questions in need of answers. Are all stars actually suns like our own, only much farther away? Could there be planets orbiting those stars and could those planets look like our own home planet, possibly even with their own unique life forms and evolutionary histories?

An attempt to explain the origin of the Solar System was made in the 18th century in part by Immanuel Kant and Pierre-Simon Laplace [**cite**], who argued for the former existence of a giant gas cloud. Slowly rotating, this cloud was suspected to have collapsed and subsequently flattened out due to its own gravitaty. Later on, the Sun and the planets were thought to have emerged from the gas.

After the invention of the first (semi-)modern telescopes by Galileo (?), the following centuries saw the discoveries of more planets in our own solar system. First Uranus in the late 1700s, then Neptune a century later, bringing the number of known planets in our solary system to eight. The discovery of Pluto and later many other objects of the same size in the outer solar system prompted the *International Astronomical Union* to formally define the term *planet* in 2006 [**cite**]. For any object in the Solar System to be classified as a planet, it has to

1. be in direct orbit around the Sun
2. possess a mass large enough to assume a nearly round shape due to self-gravitation
3. have cleared its orbit of any larger or similarly-sized bodies

With continuing scientific and technological progress, the observing distance of astronomical bodies grew drastically. Larger and more accurate telescopes, as well as the eventual possibility of launching those telescopes into orbit made the discovery of extrasolar planets feasible. The first discovery of such an exoplanet was confirmed in 1991 [**cite**] with about 5000 having been observed since then, most notably by the *Kepler Space Telescope*, with which alone about 2600 planets could be detected [**cite**] that

These recent observations show that planets are very abundant (more stars with planets than without?). It seems that 1 out of every 5 Sun-like stars has an Earth-sized planet inside the Goldilocks zone, where liquid water can exist in a stable form and therefore one of the basic requirements for life is fulfilled [**cite**]. This suggests that there could be many billions of Earth-like planets in the Milky Way alone.

The mass of observed planets ranges from about twice that of the Moon to about 30 times that of Jupiter, thus spanning multiple orders of magnitude [**cite**]. Planetary compositions depend largely on their size [**cite**]. Most planetary formation theories assume an initial buildup of a rocky core [**cite**]. From there the planet evolves either into an Earth-like terrestrial planet or into a gaseous giant similar to Jupiter. ...

Rogue planets: might be more rogue planets than stars in the Milky Way [**cite**]. ...

The processes underlying planet formation are yet to be fully explaned by science. Due to temporal limits and the vastness/complexity of this active field of study, which requires and understanding of gravity (N-body dynamics), magneto-hydro-dynamics, chemistry, radiative transfer, coagulation phyics, this bachelor's thesis can only cover a tiny portion of what there is to be said.

1.2 Protoplanetary Disks

The current scientific consensus on the origin theory of stars and planets is based on the nebular hypothesis, which states that protoplanetary disks form when large interstellar clouds of molecular gas collapse under their own gravity [**cite**].

Origin of clouds?

The collapse of a gas cloud leads to a dramatic increase of gas density, pressure and temperature at its center, which for high mass clouds results in the formation of a star. In our own Solar Sytem, this took approximately x years [**cite**]. Conforming to the law of momentum conservation, the cloud's angular velocity increases during the collapse. Also, the initially present statistical distribution of velocities averages out in favor of the clouds's net angular momentum. Since the pull of gravity inwards is only balanced by the centrifugal force along the radial direction, the cloud flattens out into a disk only supported along the z-axis by gas pressure.

The flattened cloud can be regarded as an accretion disk around the central star, which after an accretion phase of approximately x years makes up almost all ($> 99\,\%$) of the mass in the disk. Planets form from the remaining gas in orbit around the star. This gas heats up due to friction and radiates away energy, which can be observed in with submillimeter telescopes.

Figure 1.1 shows two images of protoplanetary disks that were observed at the *Atacama Large Millimeter/submillimeter Array* (ALMA). In them, multiple circular dark regions can be seen. Those are regions where the gas has partially been depleted by exchanging angular momentum with the planet.

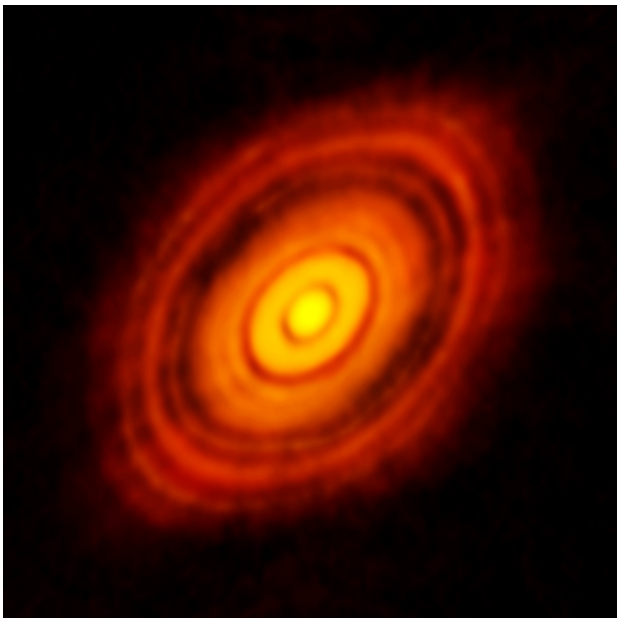

(a) Disk around *HL Tau* [**cite**]

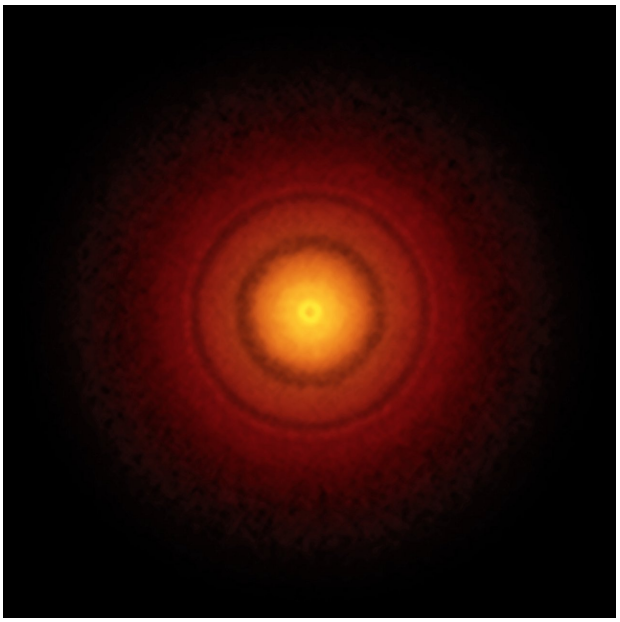

(b) Disk around *TW Hydrae* [**cite**]

Figure 1.1: Protoplanetary disks around the stars *HL Tau* and *TW Hydrae*, observed at submillimeter wavelengths with *ALMA*

To construct a simplified model of a protoplanetary disk in two dimensions, let us use cylindrical coordinates (r, φ, z). In this model, the disk is situated at $z = 0$ and infinitesimally thin. Three important attributes of the gas are its rotation, density and temperature. The trajectory of a particle of perfectly non-viscous gas in the gravitational potential of the star is described by Kepler's laws. Assuming circular orbits, the angular frequency would be

$$\Omega_K = \sqrt{\frac{GM_*}{r^3}} \tag{1.1}$$

In reality, the gas in a disk orbits its star in a non-Keplerian way. The viscosity of the gas leads to slightly lower rotation velocities.

Because the disk is much more wide then thick, it is possible to obtain a relatively accurate, yet less computationally aufwaendig model by vertically integrating the hydrodynamical equations and only working with vertically averaged state variables [**cite**]. This greatly simplifies what?.

$$\Sigma(r,t) = \int_{-\infty}^{\infty} \rho(z,t) \cdot dz \tag{1.2}$$

Millimeter observations of protoplanetary disks as of yet do not give much information about the gas density profile in the inner regions of the disk [**cite**]. Often, a power law is used:

$$\Sigma(r) = \Sigma_0 \cdot \left(\frac{r}{r_0}\right)^{-\gamma} \tag{1.3}$$

This power law is not a fact though, but an assumption. The slope of $\Sigma(r)$ is characterized by the parameter γ, which is assumed to be ≈ 1 throughout this thesis (from where?) [**cite**]. Even though the disk is treated by the FARGO2D1D algorithm as a 2D object, it is important to talk about the geometry of real disks observed in the night sky. Contrary to what one might expect without any prerequisite knowledge, observations show that a disk's width grows larger with increasing distance from the star [**cite**]. A first approximation of this can be made by expressing the width (surface scale height) H as a polynomial function of the distance from the center r.

$$H(r) = H_0 \cdot \left(\frac{r}{r_0}\right)^{\beta} \tag{1.4}$$

Here, β labels the so-called *flaring index* (observations, typical values [**cite**], cutoff radius?). This relationship suggests the definition of another useful parameter, the *aspect ratio* at radial position r

$$h_r(r) := H(r)/r \tag{1.5}$$

A typical value is 0.05 [**cite**], flaring index $= 0 \Rightarrow$ constant disk width

(a) non-flaring disk (b) flaring disk

Figure 1.2: Qualitative sketches of flaring and non-flaring disks (I'll probably replace these with a bit more detailed plots)

The chemical composition of protoplanetary disks is dominated by the contribution of molecular H_2, which in most cases makes up about 98% of the disk's mass [**cite**]. Besides that, there are also small quantities of He, Li and trace amounts of heavier elements.

Close to the central star, volatile molecules like water and methane can not exist in a stable form due to their low melting points (?). Not being able to condense into larger and heavier structures, those molecules are carried beyond the *frost line* into the outer regions of the disk by the radiation pressure of the solar wind, whereas heavier elements like metals can stay closer to the center.

The model utilized by the FARGO2D1D algorithm assumes a homogenous gas with a mean molecular mass m_{mol} [**cite**].

hydrodynamical equations, model of the disk, fluid dynamics, viscosity (also numerical viscosity?)
temperature of gas in disk relatively cool, between 10 and 10^3 K. 1×10^4 K

- isothermal equation of state (why is this accurate?)
- viscosity is assumed to be constant in time and space

$$\nu = \alpha \frac{c_s^2}{\Omega_K} \tag{1.6}$$

- local isothermal sound velocity (follows from vertical hydrostatic equilibrium)

$$c_s = H \cdot \Omega = H/R \cdot v_{Kepler} =^{?} \sqrt{\frac{kT}{\mu m_p}} \tag{1.7}$$

  give equation of state (Zustandsgleichung)

- because isothermal, gas pressure is

$$P = c_s^2 \cdot a \cdot \Sigma \tag{1.8}$$

  (equation will be used to determine gap boundaries numerically from maxima/minima in pressure gradient)

1.3 Planets in the Disk

1.3.1 Formation/Accretion Mechanisms

Most standard planet formation theories assume the initial buildup of a central rocky core [1]. From this point on, the protoplanet may either develop into a terrestrial planet or into a giant planet consisting of a rocky core and a large gaseous hull. In our own Solar System, the four terrestrial planets are those situated closest the Sun, while the four gas giants sit in the outer regions of the Solar System.

This is probably no coincidence [**cite**]. Most of the matter in the universe, and therefore most likely also in newly formed disks, consists of light elements like hydrogen and helium. Because of the radiation pressure of the solar wind, these light elements accumulate in the outer regions of the disk. Therefore, an accreting planetoid in the outskirts of the disk has much more material available for accretion in its vicinity than one close to the center.

In the early stages of planet formation, gravity does not play a dominant role. Gas and dust grains collide and stick together mainly via microphysical processes like van der Waals or Coulomb forces [6]. These processes are not still entirely understood today [**cite**]. It is unclear how the early planet cores manage to grow without fragmenting into smaller pieces again at collisions with other, similarly-sized planetesimals. This problem is called the meter-sized barrier.

The early development of planetesimals will not be studied in this thesis. It is assumed that the initial buildup of a planet core has already taken place. From this point on, the planet grows by either direct collisions with other bodies or by gravitational capture. This leads to the eventual formation of circumplanetary accretion disks similar to the protoplanetary disk itself, but on much smaller scales (how many AU approximately?)

for $\alpha = 10^{-3}$ and $H/R = 0.05$ the accumulation of mass to one Jupiter mass is on the timescale of $\approx 10^5$ a

The accreted material comes mostly from inside the planet's Hill sphere (also called Roche sphere, horseshoe region (?)) [**cite**]. This is the region in space where the gravitational influence of the planet's is larger than that of its central star [2]. If a body with mass m orbits a larger mass M with a semi-major axis a and eccentricity e, the radius of the Hill sphere can be approximated by

$$r_H \approx a(1-e)\sqrt[3]{\frac{m}{3M}} \quad \text{(why only approximately?)} \tag{1.9}$$

This thesis uses the FARGO2D1D code to simulate a protoplanetary disk, the code makes use of both a Kley and Machida accretion subroutine. For most simulations, the planet will be kept on a fixed orbit so that there is no migration.

1.3.2 Gap Formation

When sufficiently grown, the proto-planet exerts tidal torques on the disc and induces trailing spiral shocks (Lin & Papaloizou 1980, Goldreich & Tremaine 1980, and Papaloizou & Lin 1984). These transport angular momentum and material is pushed away from the proto- planet, a process which leads eventually to the opening of a gap in the disk. The detailed criteria of gap opening are given by Lin & Papaloizou (1986, 1993). The radial extent of the gap is determined by the mass of the planet, viscosity and gas pressure (Lin & Papaloizou 1993)
continued accretion through the gap [**cite**]: even after the formation of the gap, there is still accretion from regions outside or inside the planet's orbital radius ⇒ rate depends on the viscosity of the gas in the disk as well as the disk's thickness

- criteria for gap opening
- The modification of the disk density is the result of the competition of torques exerted on the disk by the planet and by the disk itself. [**crida**]
- More precisely, the planet gives some angular momentum to the outer part of the disk, while it takes some from the inner part (Lin and Papaloizou, 1979; Goldreich and Tremaine, 1980).
- However, the internal evolution of the disk, which tends to spread the gas into the void regions, opposes to the opening of the gap.
-

Chapter 2

Methods

2.1 The FARGO2D1D Algorithm

The FARGO algorithm was originally introduced by Frédéric Masset in his 1999 paper [5]. Its name is an acronym for *Fast Advection in Rotating Gaseous Objects*. The algorithm is written in *C* and utilizes a 5th order *Runge-Kutta* subroutine to determine the trajectory of a planet in the disk, as well as a fluid dynamics subroutine for the gas and accretion. (what advantages relative to other methods?)

To model a protoplanetary disk ..., it is represented in the code by a 2D grid. Each grid cell stands for a specific location in the disk. The row and column of such a cell correspond to its radial and azimuthal position.

...

In this thesis, an extension of the standard version of FARGO is utilized, titled FARGO2D1D. Here, the 2D grid is surrounded by a one-dimensional grid made of elementary rings. Far from the center, the gravitational influence of the planet on the structure of the disk is diminishingly small [4]. Because of this, the disk can be assumed to be axisymmetric for large values of r.

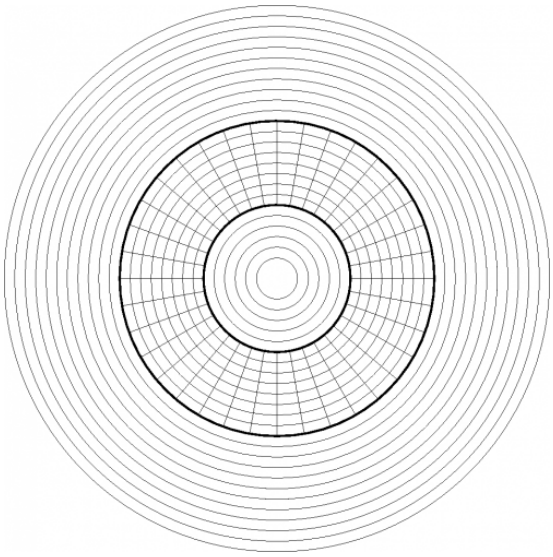

Figure 2.1: Sketch of 2D1D grid as used by the FARGO2D1D algorithm [3]

The following paragraphs will attempt to shortly summarize the most important aspects of the algorithm's inner workings.

initialization, taper, accretion wait...

ghost cells

Runge-Kutta Subroutine For Planet Motion

- n-body solver with 5th order Runge-Kutta algorithm
- family of implicit and explicit iterative methods
- developed around 1900 by German mathematicians Carl Runge and Wilhelm Kutta
- include the well-known routine called the Euler Method
-
-

Fluid Dynamics Subroutine For Gas Flow

describe

Subroutine For Gas Accretion Onto Planet

- uses both Kley and Machida
-
-
-
-

there are various different methods of modeling accretion. fargo2D1D uses a combination of Kley and Machida (maximum of both, why?). also mention others

Kley Accretion
A modified version of the accretion reciple suggested by W. Kley (1999) is used [1].

After each time step Δt, a mass amount Δm is removed from the grid cells inside the Hill sphere and added to the planet [**cite from code**].

$$m_{disk}(t + \Delta t) = m_{disk}(t) - \Delta m \tag{2.1}$$

$$m_{planet}(t + \Delta t) = m_{planet}(t) + \Delta m \tag{2.2}$$

The precise value is determined via

$$\Delta m = f_{red} \cdot S_{acc} \cdot \Sigma(r, t) \cdot f_{acc} \cdot \Delta t \tag{2.3}$$

Here, f_{red} is ..., S_{acc} is the size of the disk surface in the Hill sphere, $\Sigma(r, t)$ is the gas surface density and f_{acc} is a parameter regulating accretion rate

$$f_{red} = \begin{cases} \frac{2}{3} & \text{if } r/r_H < 0.45 \\ \frac{2}{3} \cdot \cos^4\left(\frac{r}{r_H} - 0.45\right) & \text{if } 0.45 \geq r/r_H \geq 0.95 \cdot r_H \\ 0 & \text{if } r/r_H > 0.9 \end{cases} \tag{2.4}$$

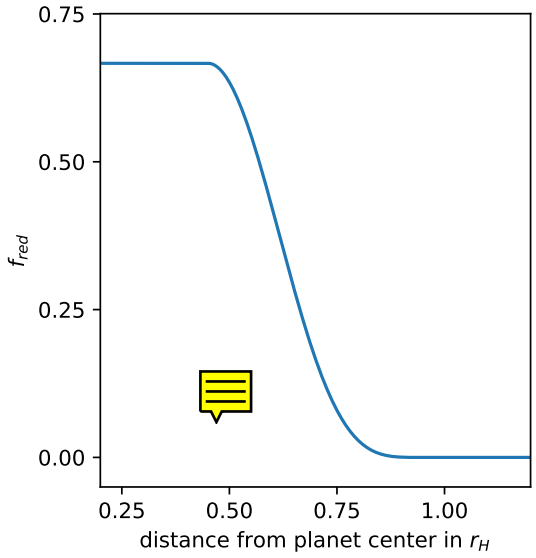

(a) r-dependence of f_{red}

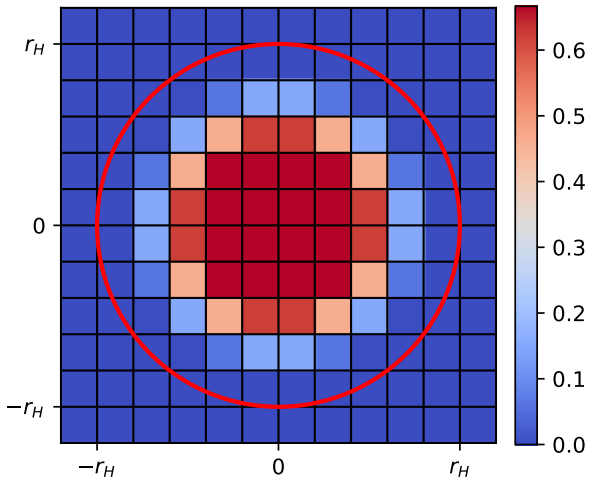

(b) Visualization of the value of f_{red} in the grid, the red circle marks the boundaries of the Hill sphere.

Figure 2.2: Smoothed step function f_{red}

Machida Accretion

$$\Delta m_M = \Sigma(r,t) \cdot H^2 \cdot \Omega \cdot \min\left(0.14;\ 0.83 \cdot (r_H/H)^{9/2}\right) \cdot \Delta t \tag{2.5}$$

- Machida et al. 2010, accretion
  runaway accretion when $m_{core} < m_{envelope}$
-

Code Units

In astronomy, one often has to deal with large numbers, e.g. the solar mass is $M_\odot \approx 1.989 \times 10^{30}\,\mathrm{kg}$. In addition to making numbers less readable and harder to work with, using large numbers may also lead to bigger numerical errors (cite). This can be avoided by choosing not to utilize SI units. Instead, a different system of measurement units is defined, which will be referenced as *code units* hereafter.

In this system, the basic measuring unit of mass is that of the sun, (i.e. $M_\odot = 1$). Spatial lengths are measured in multiples of the average distance between Jupiter and the sun, which in SI units amounts to about 5.2 au. Also, to simplify even further, the Newtonian gravitational constant G is set to unity as well.

The mass of the central star is assumed to be much larger than that of the planet. Under these assumptions, the Keplerian angular velocity is $\Omega_K = 1$ and the period of one orbit is $T = 2\pi$.

2.2 First Runs

- investigation of disk evolution, visualized as top down view on disk in polar coordinates, color coding (surface density of gas)
- one can see influence of the planet's momentum exchange with the gas
- spiral arms form
- gap forms, grows deeper with time
- TODO: explain what's going on in the center of the grid (numerical problems?)

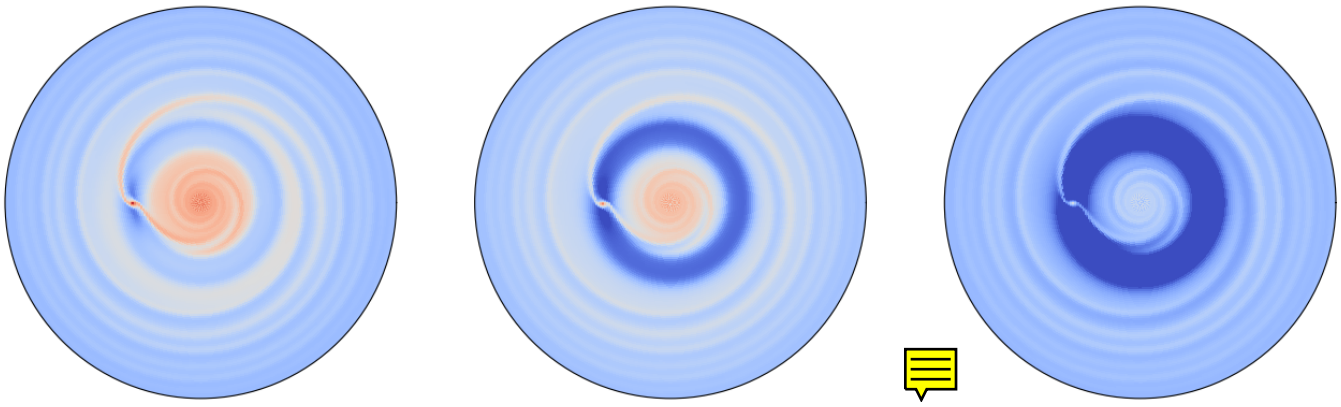

Figure 2.3: Evolution of gas surface density over time with a non-migrating planet of initial mass $m_0 = 1\ M_{jupiter}$ on a circular orbit ($\alpha_{visc} = 10^{-2},\ h_r = 0.05$)

Default Parameters
if not otherwise specified, these will be used

Table 2.1: Default parameters

aspect ratio	0.05		
flaring index	0		
$\Sigma(r=0)$	0.0003		
sigma slope	1		
α_{visc}	0.01		
Roche smoothing	0.6		
exclude Hill	yes		
mass taper	50	$e_0 = e(t=0)$	0
N_{rad}	202	$m_0 = m(t=0)$	0.001
N_{sec}	456	$m_{core,0}$	0.0003
R_{min}	0.2	accretion factor	1
R_{max}	5	acc waiting time	500
$R_{min,1D}$	0.02		
$R_{max,1D}$	50		
eccentricity	0		
skip category called "other"			
N_{tot}	2500		
N_{interm}	50		
Δt	2π		

2.3 Choosing the Resolution of the 2D1D-Grid

The FARGO2D1D algorithm defines resolution via the two variables N_{rad} and N_{sec}, which designate the number of grid cells in radial and azimuthal direction, respectively. To find the optimal simulation resolution, a compromise has to be found between the integration time and the accuracy of the simulation results. before we do this, ...

The grid is treated by the algorithm simply as a 2D rectangular matrix. In reality though, the system is of course not rectangular, but circular. The projection of the rectangular grid into polar coordinates leads to a distortion of the square grid cells. The grid cells that are very close to the center as well as those very far away from the center are subject to strong distortions.

To make sure that the accretion subroutine functions accurately, the resolution should be chosen in such a way that the grid cells' shape is as close to a square as possible at the radial position of the planet. For that, let's take a look at Figure 2.4, which visualizes a radial grid section at a distance r from the center.

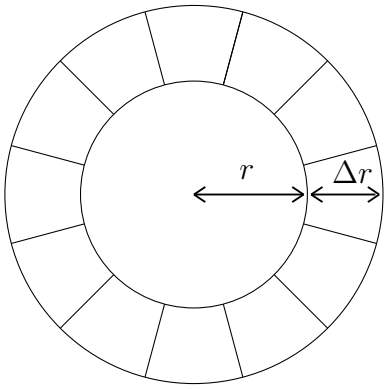

Figure 2.4: Sketch of a radial division in the simulation grid

To be as close to a square as possible, each azimuthal division should ideally have an area of

$$A_{cell} \approx \Delta r^2 \tag{2.6}$$

The total area of the ring is given by

$$A_{ring} = \pi(r + \Delta r)^2 - \pi r^2 = \pi(2r\Delta r + \Delta r^2) \tag{2.7}$$

Utilizing the relation $N_{sec} = A_{ring}/A_{cell}$ and then plugging in $r = 1$, this yields

$$N_{sec} = \pi\left(\frac{2}{\Delta r} + 1\right) \tag{2.8}$$

where the width of the ring is related to the radial resolution N_{rad} via

$$\Delta r = \frac{r_{max} - r_{min}}{N_{rad}} \tag{2.9}$$

Here, r_{min} and r_{max} denote the inner and outer radial boundaries of the 2D grid. They are set to $r_{min} = 0.2$ and $r_{max} = 5$, respectively. It should now be clear how to easily calculate the optimal value of N_{sec} for any value of N_{rad}. Still, a few test simulations need to be run before one can decide on the resolution which optimizes the trade-off between integration time and accuracy.

Simulations are to be run for multiple different resolutions, namely 2.5, 5 and 10 cells per Hill radius. For each number $N_{c/rH}$ of cells per Hill radius, N_{rad} can be calculated via

$$N_{rad} = N_{c/rH} \cdot \frac{r_{max} - r_{min}}{r_H} \tag{2.10}$$

From this, N_{sec} can be determined with Equation 2.8 and Equation 2.9. This leads to the following values for the radial and azimuthal resolutions:

Table 2.2: caption

cells per r_H	N_{rad}	N_{sec}
2.5	101	230
5	202	456
10	404	909

Figure 2.5 visualizes how the planet's Hill sphere is implemented in the 2D array. For the simulations, a planet on a circular orbit with an intitial mass of 1 $M_{jupiter}$ is used, which builds up during a taper period of 10 orbits. After these 10 orbits, the planet starts accreting mass from its surroundings.

The radial gas density profile after a total of 500 orbits can be seen in Figure 2.6. There is some discrepancy for small radii, but the overall structure of the gas density profile seems to be pretty much the same. To look at the behavior near zero, Figure 2.7 shows a zoomed in view of the disk. As can be seen here, a resolution of 2.5 cells per Hill radius leads to artifacts near the center. Because of this, a resolution of 5 cells per r_H is chosen. If not otherwise specified, all following simulations are run with

$$N_{rad} = 202 \text{ and } N_{sec} = 456$$

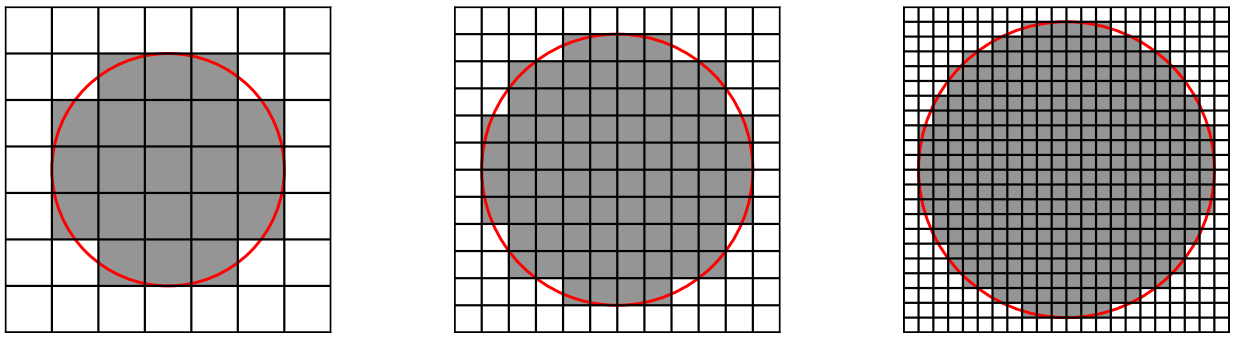

(a) 2.5 cells per r_H (b) 5 cells per r_H (c) 10 cells per r_H

Figure 2.5: Hill spheres in the grid for various resolutions

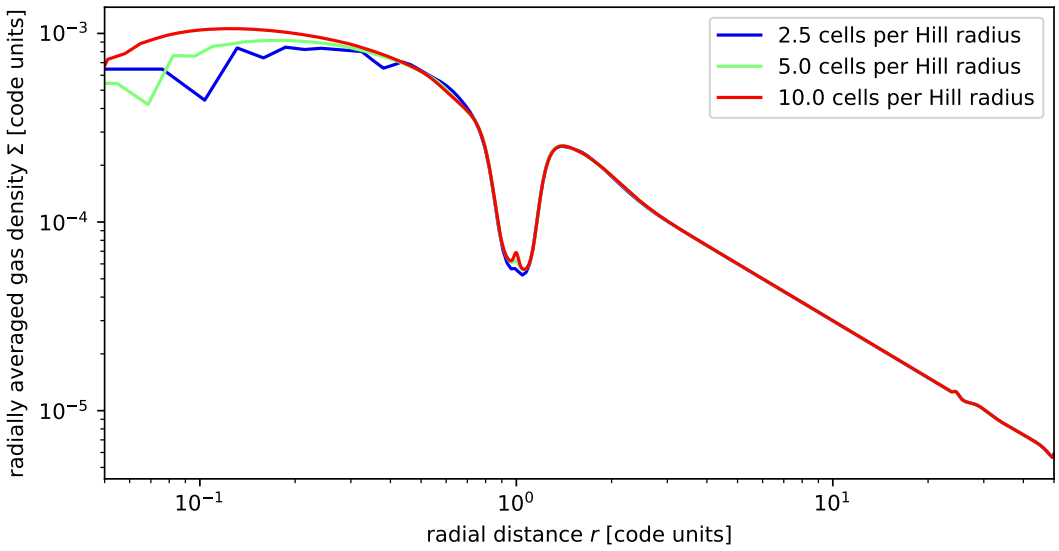

Figure 2.6: Azimuthally averaged gas densities for different resolutions ($\alpha_{visc} = 10^{-2}$, $h_r = 0.05$). The planet is initialized on a circular orbit with $m_0 = 1\ M_{jupiter}$ and in total performs 500 orbits, with a taper period of 5 orbits and an accretion wait time of 10 orbits. The general structure of the gas density follows approximately the same course for all resolution values, with discrepancies being the largest for small values of r.

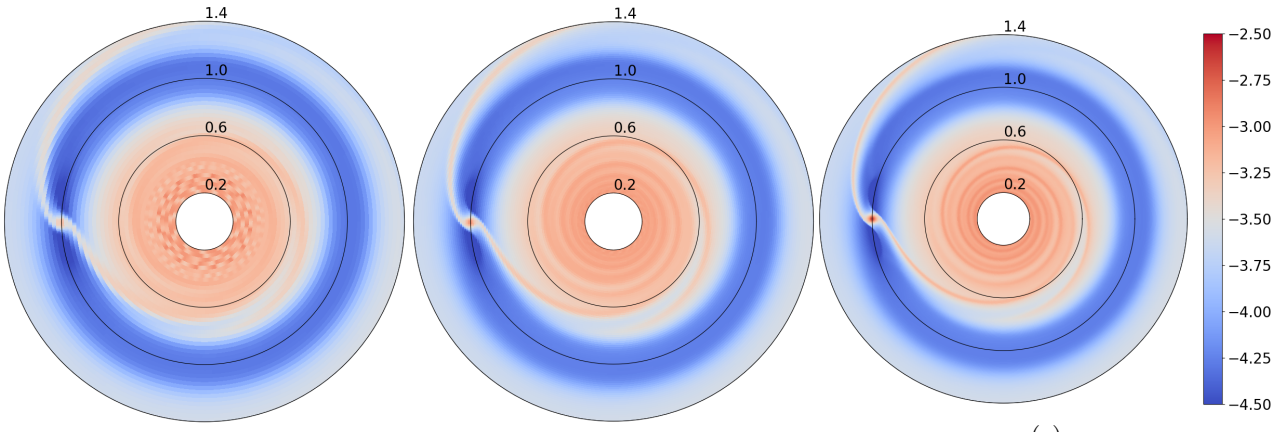

(a) (b) (c)

Figure 2.7: Logarithmic gas density in the inner regions of the grid for different resolutions. The black rings show the distance from the center, the color bar displays the order of magnitude (decadic logarithm) of the gas density in code units. For the lowest resolution, artifacts can be observed near the center of the disk.

2.4 Parameter Studies of the Disk

In this section, the influence of various parameters of the disk on the planet's accretion rate and gap structure is investigated. This is done for the disk's aspect ratio, radial gas profile and gas viscosity.

2.4.1 Aspect Ratio and Flaring Index of the Disk

- gap can't form for large values of h_r
- accretion increases linearly with h_r, i.e. with disk width
  $\Rightarrow$ makes sense, more material available

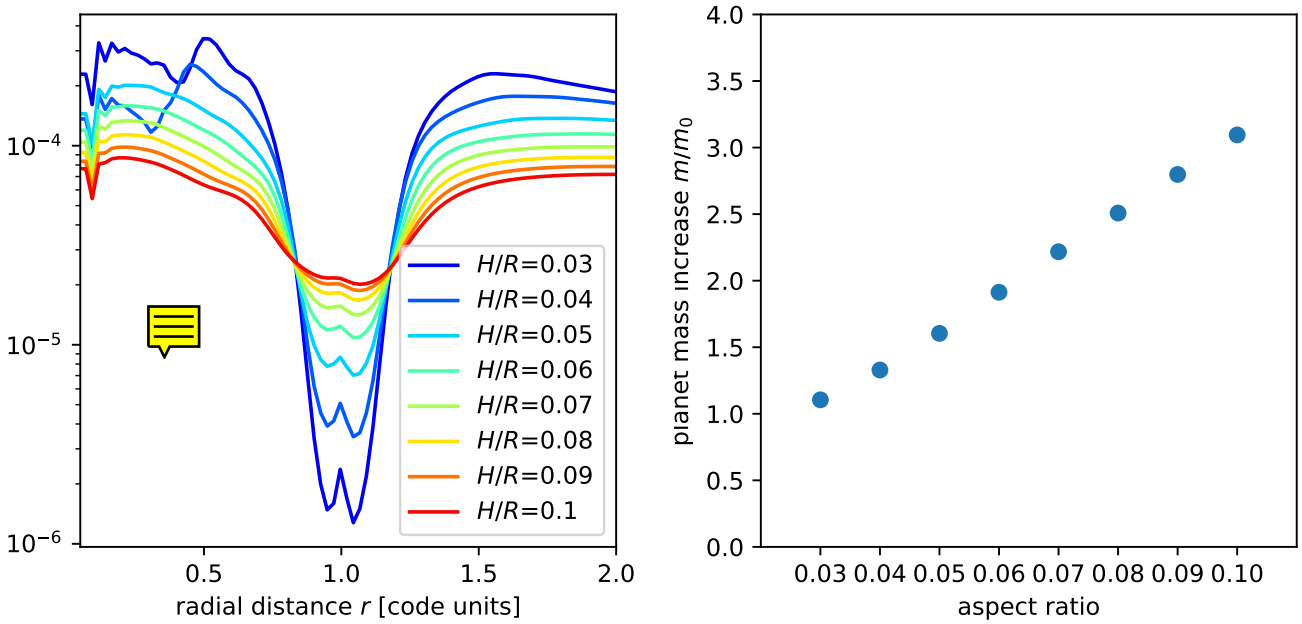

(a) radial gas density after 2500 orbits vs. aspect ratio (b) relative mass increase over time vs. aspect ratio

Figure 2.8: Influence of aspect ratio h_r on gap profile and planet's relative mass increase. The planet is initialized on a circular orbit with $m_0 = 1\ M_{jupiter}$, a tapering period of 50 orbits, 500 orbits of accretion wait time and 2500 orbits in total. Disk viscosity is $\alpha_{visc} = 10^{-2}$.

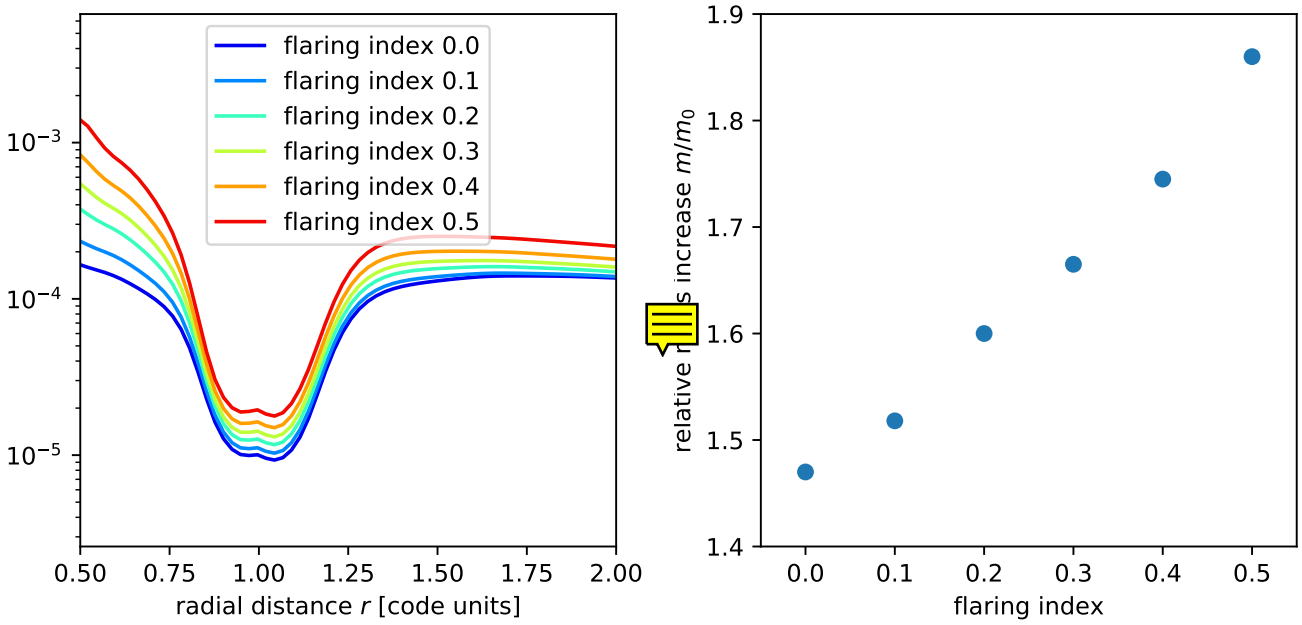

(a) radial gas density vs. flaring index

(b) relative mass increase vs. flaring index

Figure 2.9: Influence of flaring index on gap profile and planet's relative mass increase. The planet is initialized on a circular orbit with $m_0 = 1\ M_{jupiter}$, a tapering period of 50 orbits, 500 orbits of accretion wait time and 2500 orbits in total. Disk viscosity is $\alpha_{visc} = 10^{-2}$ and aspect ratio is $h_r = 0.05$.

2.4.2 Gas Viscosity Parameter

- accretion increases with α, not linear (why)
- gap doesn't form for large α
- numerical viscosity (removed the data point for $\alpha_{visc} < 10^{-4}$)

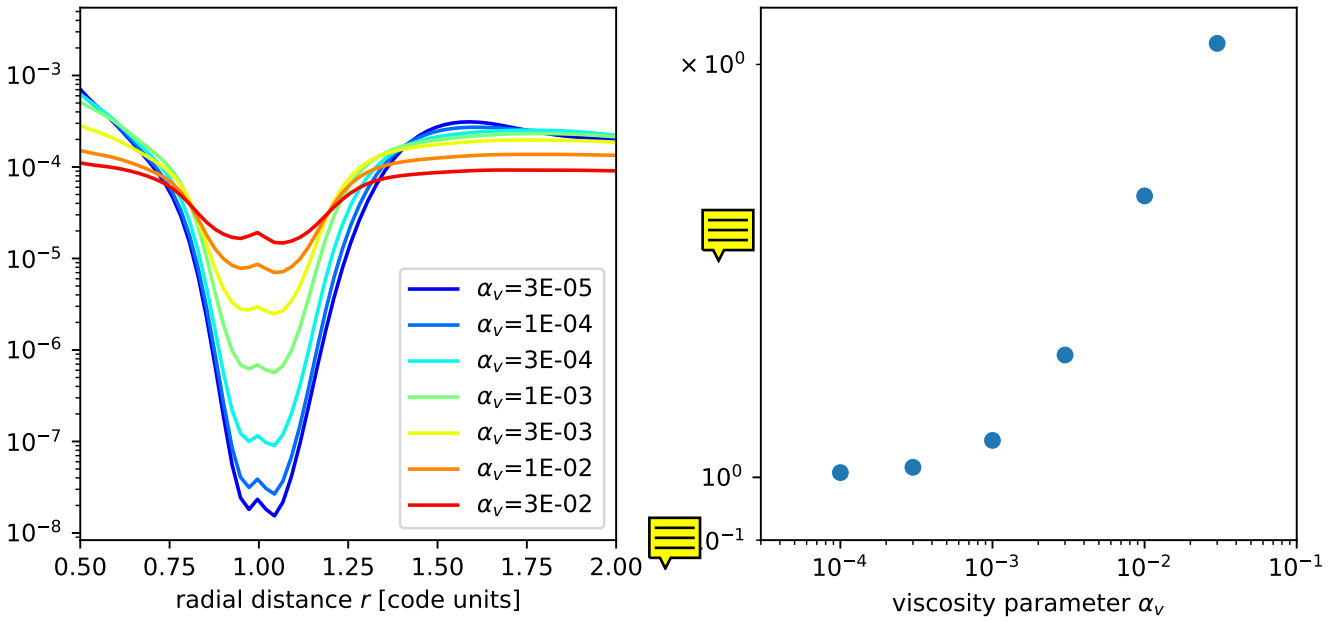

(a) radial gas density vs. flaring index

(b) relative mass increase vs. flaring index

Figure 2.10: Influence of gas viscosity on gap profile and planet's relative mass increase. The planet is initialized on a circular orbit with $m_0 = 1\ M_{jupiter}$, a tapering period of 50 orbits, 500 orbits of accretion wait time and 2500 orbits in total. The aspect ratio is $h_r = 0.05$.

2.5 Parameter Studies of a Planet in the Disk

2.5.1 Initial Planet Mass

- smaller planets accrete faster (relative to initial mass)
  ⇒ makes sense, larger planets open gap faster/wider

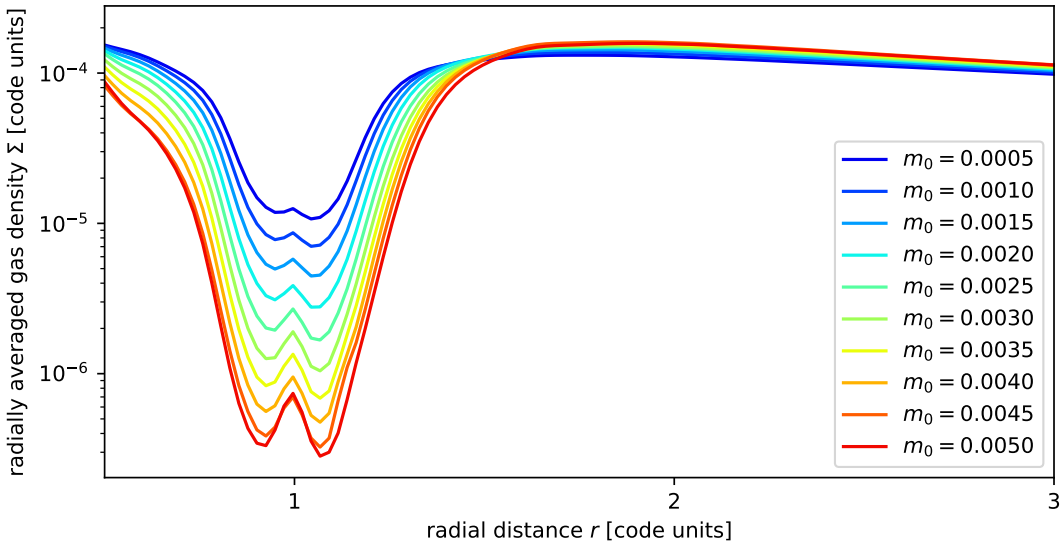

Figure 2.11: radial gas density after 2500 orbits vs. initial planet mass

Figure 2.12: Influence of a planet's initial mass on the gap profile. The planet is initialized on a circular orbit with $m_0 = 1\ M_{jupiter}$, a tapering period of 50 orbits, 500 orbits of accretion wait time and 2500 orbits in total. The aspect ratio is $h_r = 0.05$.

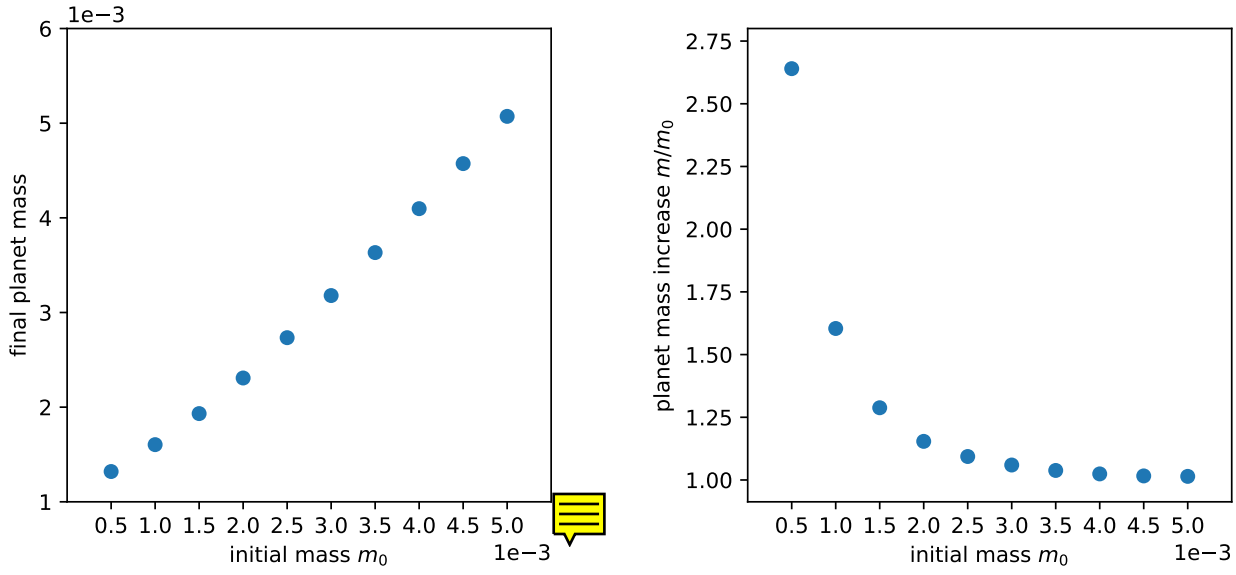

(a) absolute mass

(b) relative mass increase m/m_0

Figure 2.13: Influence of initial mass on a planet's absolute and relative mass increase. The planet is initialized on a circular orbit with a tapering period of 50 orbits, 500 orbits of accretion wait time and 2500 orbits in total. The aspect ratio is $h_r = 0.05$ and the viscosity $\alpha_{visc} = 0.05$.

2.5.2 Accretion rate Machida Accretion Factor

- relative planet mass increase grows with accretion factor (obviously, makes sense)
- there is an upper limit, gap forms, horse show region depletes
  ⇒ accretion limited by gas inflow (disk viscosity)

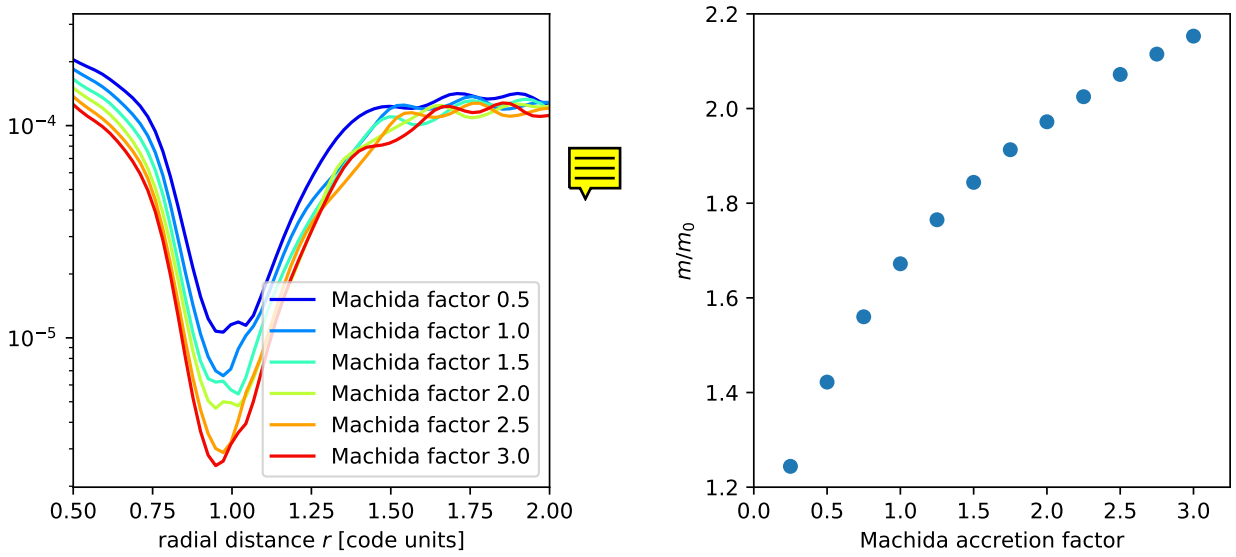

(a) radial gas density vs. Machida accretion factor (b) relative mass increase vs. Machida accretion factor

Figure 2.14: Influence of the accretion rate on the gap profile and the planet's relative mass increase. The planet is initialized on a circular orbit with $m_0 = 1\ M_{jupiter}$, a tapering period of 50 orbits, 500 orbits of accretion wait time and 2500 orbits in total. The aspect ratio is $h_r = 0.05$ and the viscosity $\alpha_{visc} = 0.05$.

2.5.3 Initial Planet Eccentricity

2500 orbits

- gap is wider/less deep for higher eccentricities
- accretion is faster for higher eccentricities
- TODO: compare with plot accretion rate vs. eccentricity (at T=2500 orbits)

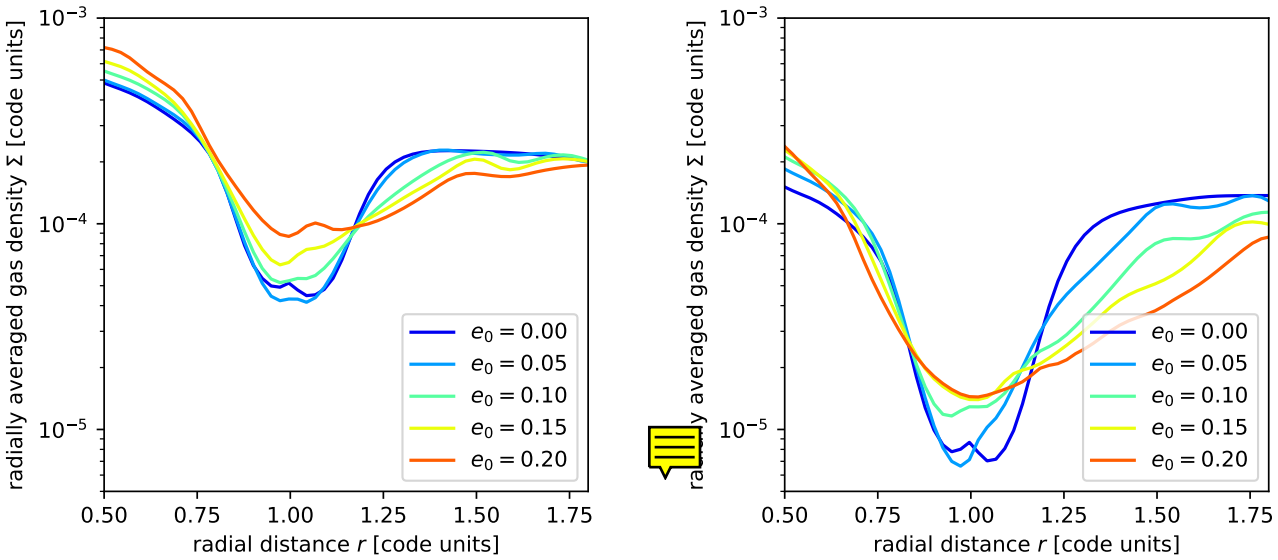

(a) before accretion ($T = 500$ orbits)

(b) after accretion ($T = 2500$ orbits)

Figure 2.15: Influence of the initial eccentricity of a planet on the gap profile. The planet is initialized with $m_0 = 1\ M_{jupiter}$, a tapering period of 50 orbits, 500 orbits of accretion wait time and 2500 orbits in total. The aspect ratio is $h_r = 0.05$ and the viscosity $\alpha_{visc} = 0.05$.

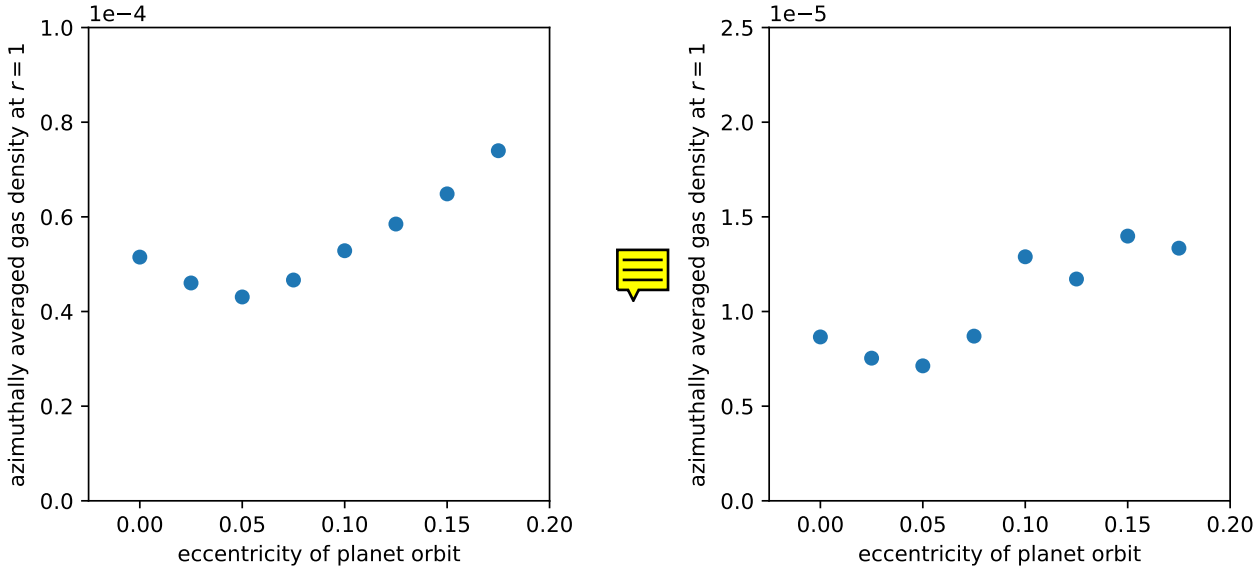

(a) before accretion $T = 10$ orbits

(b) after accretion ($T = 50$ orbits)

Figure 2.16: Influence of the initial eccentricity of a planet on the depth of the gap at the position of the planet, i.e. $\Sigma(r = 1)$. The planet is initialized with $m_0 = 1\ M_{jupiter}$, a tapering period of 50 orbits, 500 orbits of accretion wait time and 2500 orbits in total. The aspect ratio is $h_r = 0.05$ and the viscosity $\alpha_{visc} = 0.05$.

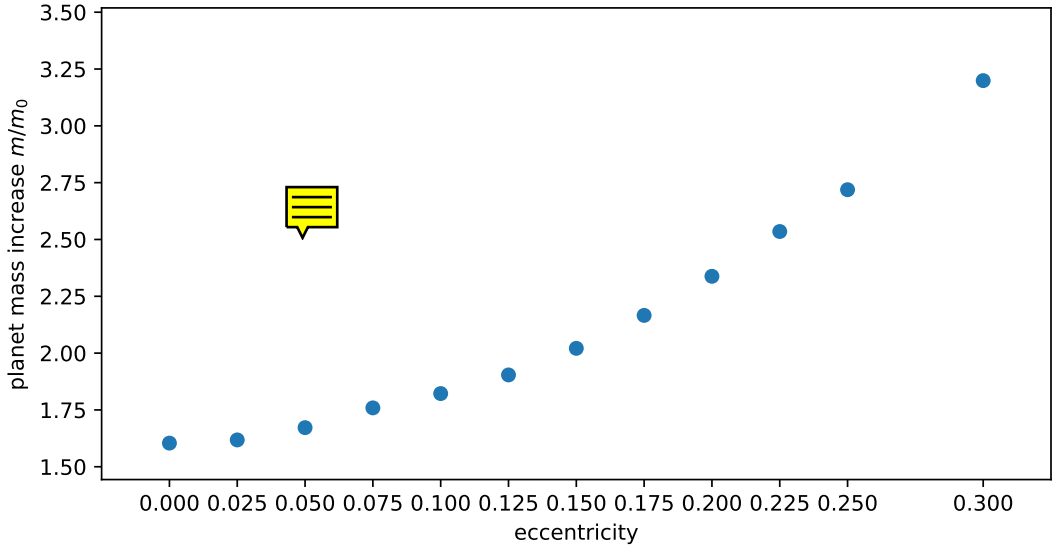

Figure 2.17: Influence of the initial eccentricity of a planet on relative mass increase. The planet is initialized with $m_0 = 1\ M_{jupiter}$, a tapering period of 50 orbits, 500 orbits of accretion wait time and 2500 orbits in total. The aspect ratio is $h_r = 0.05$ and the viscosity $\alpha_{visc} = 0.05$.

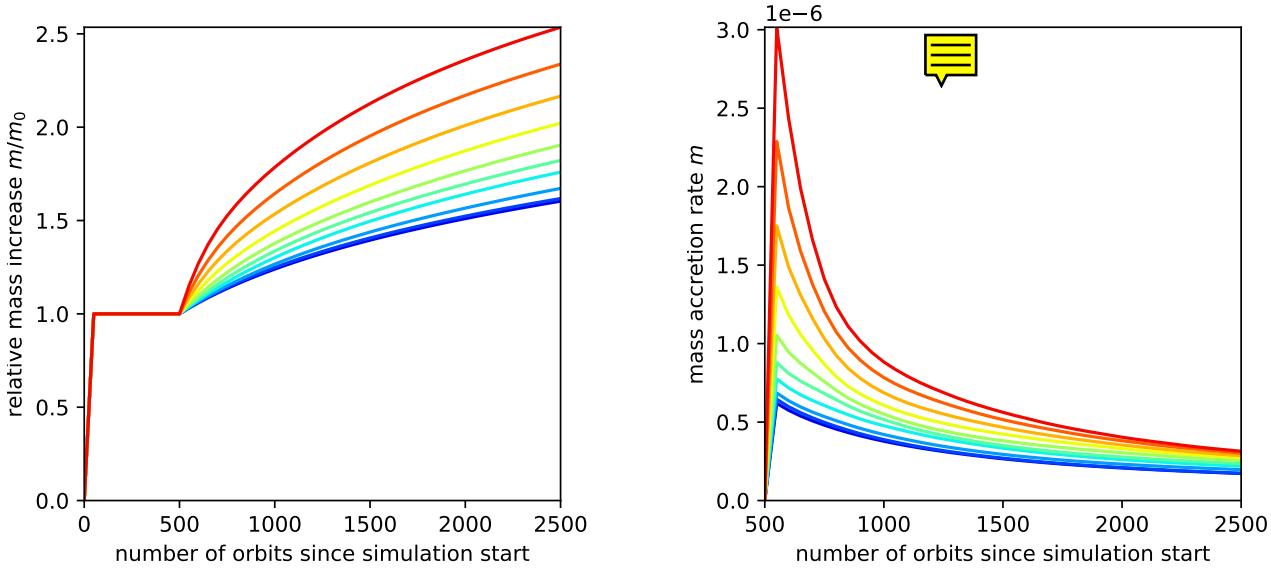

(a) relative mass increase vs. time and e_0

(b) accretion rate vs. time and e_0

Figure 2.18: Influence of the initial eccentricity of a planet on relative mass increase and accretion rate over time. The planet is initialized with $m_0 = 1\ M_{jupiter}$, a tapering period of 50 orbits, 500 orbits of accretion wait time and 2500 orbits in total. The aspect ratio is $h_r = 0.05$ and the viscosity $\alpha_{visc} = 0.05$. (add a colorbar)

- long term evolution (50000 orbits)
- accretion rates converge to a value that is determined by the speed with which gas flows back into the gap (⇒ viscosity)

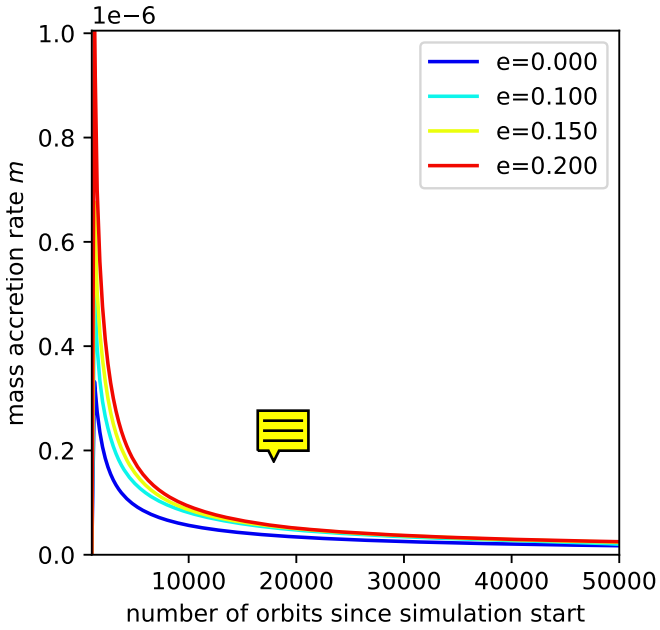

Figure 2.19: Influence of the initial eccentricity of a planet on relative mass increase and accretion rate over a longer time. The planet is initialized with $m_0 = 1\ M_{jupiter}$, a tapering period of 50 orbits, 1000 orbits of accretion wait time and 50000 orbits in total. The aspect ratio is $h_r = 0.05$ and the viscosity $\alpha_{visc} = 0.05$. (maybe zoom in & determine limiting value?

Gap Eccentricity

- gap boundaries can be calculated from minima and maxima of the gas pressure in the disk
- eccentricity can be calculated from semimajor and semiminor axes a and b

$$e = \frac{a+b}{a-b} \tag{2.11}$$

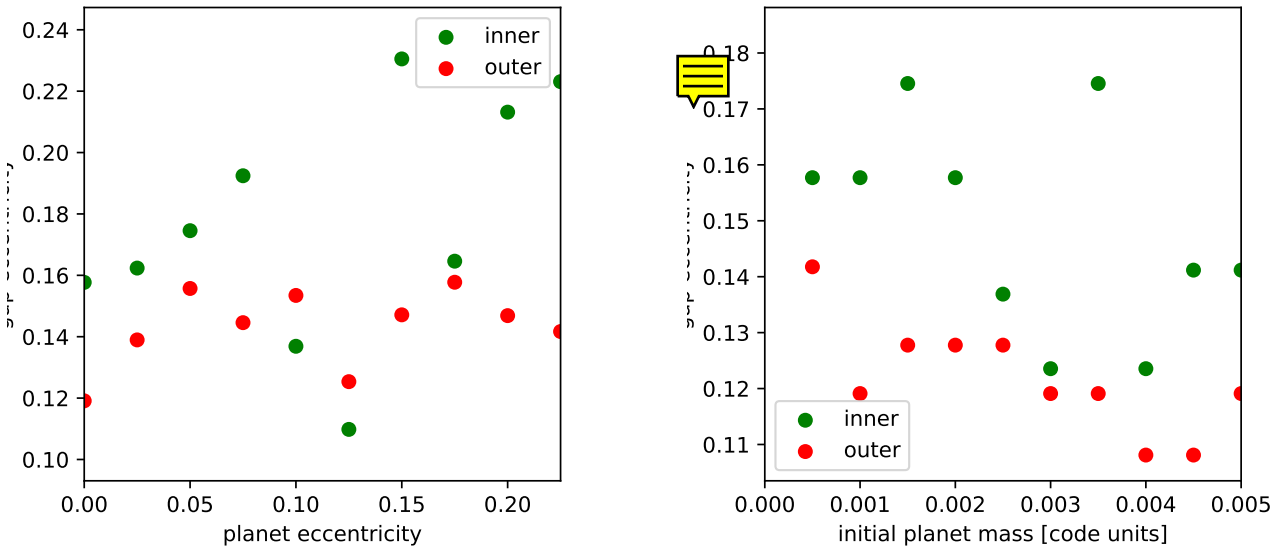

(a) gap eccentricity vs. initial planet eccentricity

(b) gap eccentricity vs. initial planet mass

Figure 2.20: Influence of the initial eccentricity and mass of a planet on the eccentricity of the gap. The planet is initialized with $m_0 = 1\ M_{jupiter}$, a tapering period of 50 orbits, 500 orbits of accretion wait time and 2500 orbits in total. The aspect ratio is $h_r = 0.05$ and the viscosity $\alpha_{visc} = 0.05$. (something seems to be wrong with the way I determine gap boundaries from pressure gradients, still needs to be fixed)

Migration

- plot eccentricity vs. time

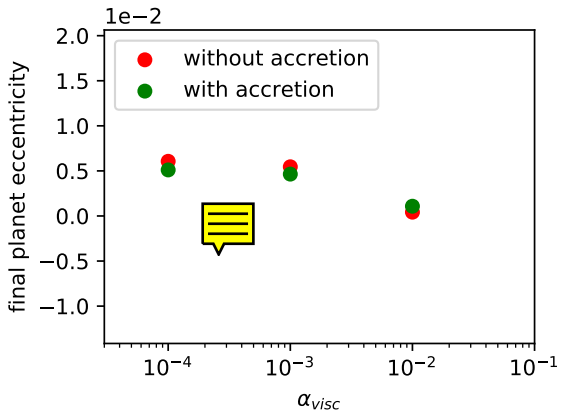

(a) final eccentricity vs. α_{visc}

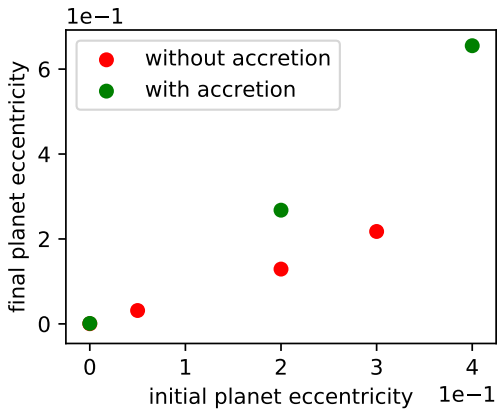

(b) final eccentricity vs. initial planet eccentricity

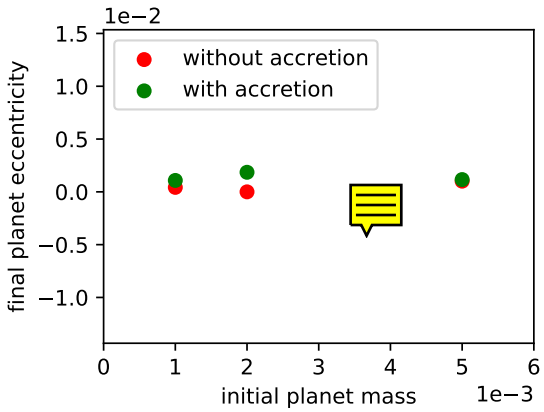

(c) final eccentricity vs. initial planet mass

Figure 2.21: Influence of the gas viscosity, initial eccentricity and mass of a planet on the final eccentricity after a migration period. The planet is initialized with $m_0 = 1\ M_{jupiter}$, a tapering period of 50 orbits, 500 orbits of accretion wait time and 2500 orbits in total. The aspect ratio is $h_r = 0.05$ and the viscosity $\alpha_{visc} = 0.05$. (rerun: without accretion until 500 orbits, then with accretion turned on)

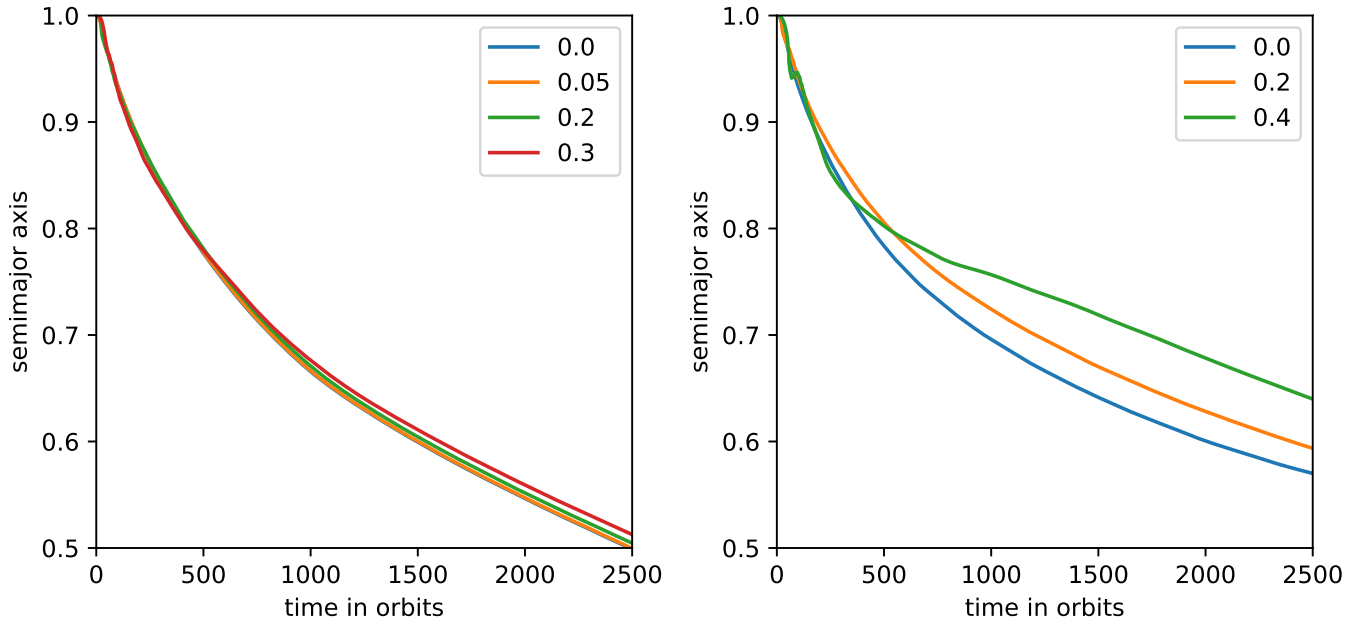

(a) without accretion (b) with accretion

Figure 2.22: Temporal evolution of the semimajor axis of a migrating planet. The planet is initialized with $m_0 = 1\ M_{jupiter}$ for various eccentricities. The tapering period is 50 orbits, accretion wait time is 500 orbits and total integration time is 2500 orbits. The aspect ratio is $h_r = 0.05$ and the viscosity $\alpha_{visc} = 0.05$. (ignore content of plots for now, need to be rerun)

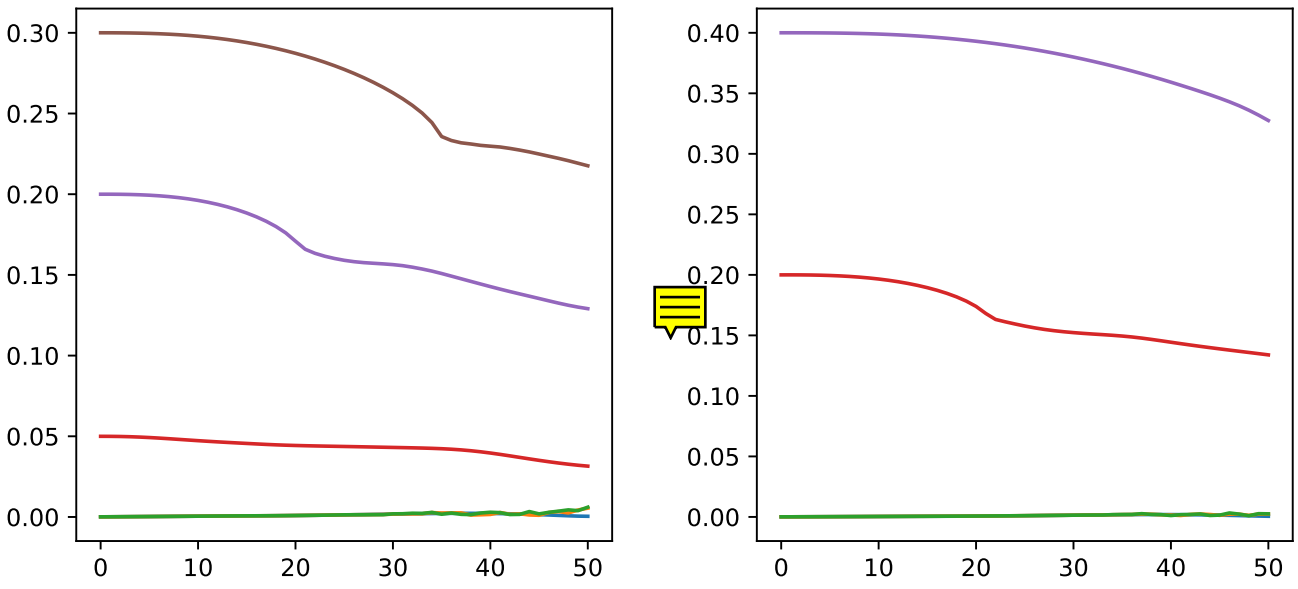

(a) without accretion (b) with accretion

Figure 2.23: Temporal evolution of the eccentricity of a migrating planet. The planet is initialized with $m_0 = 1\ M_{jupiter}$ for various eccentricities. The tapering period is 50 orbits, accretion wait time is 500 orbits and total integration time is 2500 orbits. The aspect ratio is $h_r = 0.05$ and the viscosity $\alpha_{visc} = 0.05$. (ignore content of plots for now, need to be rerun)

Chapter 3

Results

- investigation: effect of planet eccentricity on accretion rate
- various disk parameter's influence on gap formation
- influence of gap on accretion rate

Chapter 4

Discussion

- compare to planet population synthesis (Bitsch 2018)
  von wem war nochmal das andere Paper? das hier?
  `http://www.mpia.de/homes/ppvi/chapter/benz.pdf`
-
-
-
-

Chapter 5

Appendix

5.1 References

[1] Kley et. al. "Mass flow and accretion through gaps in accretion discs". In: *Monthly Notices of the Royal Astronomical Society* 303.4 (1999), pp. 696–710. DOI: 10.1046/j.1365-8711.1999.02198.x.

[2] D.P. Hamilton & J.A. Burns. "Orbital stability zones about asteroids. II - The destabilizing effects of eccentric orbits and of solar radiation". In: *Icarus* 96.1 (1992), pp. 43–64. DOI: https://www.sciencedirect.com/science/article/pii/001910359290005R.

[3] FARGO3D. *2D1D grid*. [Online; accessed January 06, 2020]. URL: http://fargo.in2p3.fr/local/cache-vignettes/L500xH501/gif_1D2Dgrid-352ab.png.

[4] FARGO3D. *What is FARGO2D1D?* URL: http://fargo.in2p3.fr/What-is-FARGO-2D1D. (accessed: 17.01.2020).

[5] Frederic Masset. "FARGO: a fast eulerian transport algorithm for differentially rotating disks". In: *Astron. Astrophys. Supp. Series* (1999). DOI: 10.1051/aas:2000116.

[6] William R. Ward. "Planetary Accretion". In: *Completing the Inventory of the Solar System, Astronomical Society of the Pacific Conference Proceedings* 107 (1996), pp. 337–361. DOI: 1996ASPC..107..337W.

5.2 Abbreviations

ALMA Atacama Large Millimeter/submillimeter Array

Declaration

Ich versichere, dass ich diese Arbeit selbstständig verfasst und keine anderen als die angegebenen Quellen und Hilfsmittel benutzt habe.

Heidelberg, den ...,